JOURNAL OF BACTERIOLOGY, Sept. 1986, p. 935–939
0021-9193/86/090935-05$02.00/0

Vol. 167, No. 3

Electron Probe Analysis, X-Ray Mapping, and Electron Energy-Loss Spectroscopy of Calcium, Magnesium, and Monovalent Ions in Log-Phase and in Dividing *Escherichia coli* B Cells

CHUNG-FU CHANG,† HENRY SHUMAN, AND ANDREW P. SOMLYO*

Pennsylvania Muscle Institute, University of Pennsylvania School of Medicine, Philadelphia, Pennsylvania 19104

Received 3 March 1986/Accepted 27 May 1986

The elemental composition of individual cells of rapidly frozen and cryosectioned *Escherichia coli* B was measured with electron optical microanalytic methods. The Ca content was high (26.2 mmol/kg) in a 10-nm-wide region of the cell envelope. Amounts of cytoplasmic Ca in actively dividing cells were significantly higher (32.6 mmol/kg [dry weight]) than in the log-phase (1.5 mmol/kg) cells. Cellular Mg was 205 mmol/kg (dry weight) and it was uniformly distributed throughout the cell. Cells washed in distilled water before freezing lost monovalent ions (Na, Cl, and K), but the membrane-bound Ca and cellular Mg were not reduced, indicating that cellular Mg and membrane Ca are more tightly bound.

The ability of bacteria to actively transport and concentrate inorganic ions is well known (11, 19), but uncertainty exists about their intracellular distribution and exchange ability. For example, recent authors (17) found that the Mg content of *Escherichia coli* is higher than had been previously reported (14, 16) and suggested that it was bound to DNA in the nucleoid. Until now, bacterial electrolytes have been measured with bulk chemical methods, primarily atomic absorption spectroscopy. However, with such methods, it is not possible to determine the intracellular distribution and proportion of membrane-bound ions nor to detect fluxes in putative ionic messengers, such as Ca^{2+}, that may occur in a small proportion of a partially synchronized population. In contrast, electron probe microanalysis (EPMA), X-ray mapping, and electron energy loss spectroscopy (EELS) of ultrathin cryosections are techniques uniquely suitable for measuring the subcellular concentration and distribution of various elements (28) and have been used previously to demonstrate the distribution of calcium and other elements in bacterial spores (1, 30, 31). We used these latter methods to quantitate and determine the subcellular distribution of Mg^{2+}, Ca^{2+}, Na^+, K^+, and other elements (P, S, and Cl) in *E. coli*. In addition to these measurements of cell composition and elemental distribution, we demonstrated the high Ca concentration in *E. coli* envelopes and showed that the cytoplasmic Ca^{2+} was increased in dividing cells. A preliminary report of some of these findings has been published (4).

MATERIALS AND METHODS

Growth of cells. *E. coli* B cells were inoculated at a temperature of 37°C into 125 ml of synthetic medium containing 0.19 mM Mg^{2+} (17). The doubling time of the cells was 30 min. To prepare log-phase cells, shaking of the bacterial culture was stopped at 3×10^8 cells per ml after 3 h. All the cell cultures were centrifuged (10,000 rpm for 10 min at 4°C) to prevent ion redistribution due to changes in cell metabolites and cell pH. Washed cells were also prepared as follows: the culture was washed twice, at 4°C for 10 min each time, with deionized distilled water; all of the centrifuge tubes, with a pellet in each, were maintained at 4°C for about 2 min before freezing.

Rapid freezing. The centrifuged pellets were scraped with a spatula, and the material was transferred from the spatula to a bamboo stick 0.4 mm in diameter. Upon transferring the material onto the stick, the stick was immediately frozen by plunging it manually into supercooled Freon 22 (E. I. du Pont de Nemours & Co., Inc., Wilmington, Del.) at −164°C. Frozen specimens were sectioned and were freeze-dried as described in detail by Somlyo and Silcox (29). A schematic diagram of the experiment described above is shown in Fig. 1.

A representative electron micrograph of a cryosection of a dense region of a pellet is shown in Fig. 2a, and images of freeze-substituted bacteria (the latter not used for analysis) are shown in Fig. 2b. The latter specimen was frozen as was the earlier sample, but after freezing it was substituted with ethanol at −80°C and infiltrated with Lowicryl HM-20 at −35°C, following the protocol provided by the manufacturer (Chemische Werke Lowi). While the components of the cell envelope can be resolved (9) in the freeze-substituted preparation, they are not distinguishable in the unstained cryosections. The in vivo elemental composition was not reflected in the freeze-substituted specimens, and thus they were not used for analysis. Therefore, we refer to the outermost, approximately 50-nm region of the cell as the cell envelope.

All of the quantitative analyses, EPMAs, and EELS were performed with an EM 400 electron microscope (EM) equipped with a field emission gun, with a scanning-transmission electron microscopy (STEM) attachment (Philips Electronic Inst., Mahwah, N.J.), and with a liquid-nitrogen-cooled specimen holder (Gatan Inc., Warrandale, Pa.) operated at a temperature of −101°C. However, for X-ray mapping, a low-background specimen holder (Philips) was used (at room temperature) to maximize stage stability.

EPMA. The microscope was operated in the transmission mode. Depending upon the orientation of *E. coli* cells when they were sectioned, the cells had various shapes and sizes. Criteria for dividing cells were a length of 3 μm or more and a distinct constriction in the cell envelope. The probes for cytoplasmic analysis were defocused to be as large as

* Corresponding author.
† Present address: Department of Biochemistry, University of Arizona, Tucson, AZ 85721.

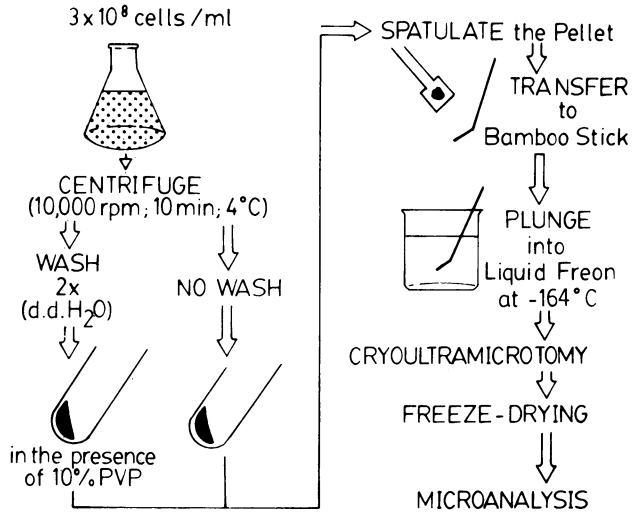

FIG. 1. Schematic drawing of the specimen preparation.

possible (approximately 0.2 μm) without overlapping the cell envelope, while the probes used for cell envelope analysis were focused to approximately 60 nm, so most of the signal originated from the cell envelope. The X rays were recorded with a 30-mm detector (Kevex Corp., Analytical Instruments, Foster City, Calif.) and multichannel analyzer (Kevex) interfaced with a PDP11/34 computer. Spectra were collected from each domain of the cell during an analysis time (typically 100 s) required to reach a measurement error (standard deviation of the calcium concentration) of less than 3 mmol/kg (dry weight). The procedure used to quantify elemental concentrations from the X-ray spectrum has been described in detail previously (12, 24). Radiation damage-induced mass loss from organic specimens under these analytical conditions is approximately 20% (24) and is equivalent to the added mass of the carbon support films.

X-ray mapping. The X-ray mapping of elements (Mg, P, and Ca) was performed with the microscope in the STEM mode at a magnification of ×50,000. The corresponding picture element (pixel) size was approximately 16 nm. A minicomputer (DeAnza VC5000; Gould, Inc., Fairfax, Va.) interfaced with the STEM to control the electron beam location (13). X-ray spectra were collected at each pixel with a dwell time of 10 s per pixel. The elemental concentrations (Mg, P, and Ca) at each pixel were quantitated by multiple least-squares fitting to characteristic peaks of these elements (12). The X-ray map of a specific element is a two-dimensional display of its concentration, proportionate to the ratio of characteristic and continuum X-ray counts at each pixel. The array sizes were 32 × 32 pixels for both transverse and longitudinal sections. Displayed images were processed with a (three-point interpolation) smoothing algorithm.

TABLE 1. Elemental concentrations of log-phase *E. coli* B

Element or ion	Concn (mmol/kg [dry wt] ± SEM)			
	Cytoplasm		Cell envelope	
	In medium (n = 28)	Washed[a] (n = 25)	In medium (n = 25)	Washed (n = 20)
Na	401 ± 22.2	123 ± 22.7	377 ± 26.2	81 ± 9.7
Mg	205 ± 10.0	281 ± 11.3	110 ± 8.0	131 ± 10.1
P	1,226 ± 42.4	154 ± 98.8	995 ± 30.6	997 ± 20.6
S	172 ± 5	140 ± 8.3	158 ± 4.9	123 ± 6.2
Cl	246 ± 19.7	27 ± 2.1	221 ± 14.3	14 ± 1.4
K	576 ± 34.6	296 ± 31.3	483 ± 29.8	166 ± 14.4
Ca	1.5 ± 0.6	6.9 ± 0.9	26.2 ± 1.2	26.2 ± 1.4

[a] Cells were washed in distilled H_2O at 4°C, as described in the text.

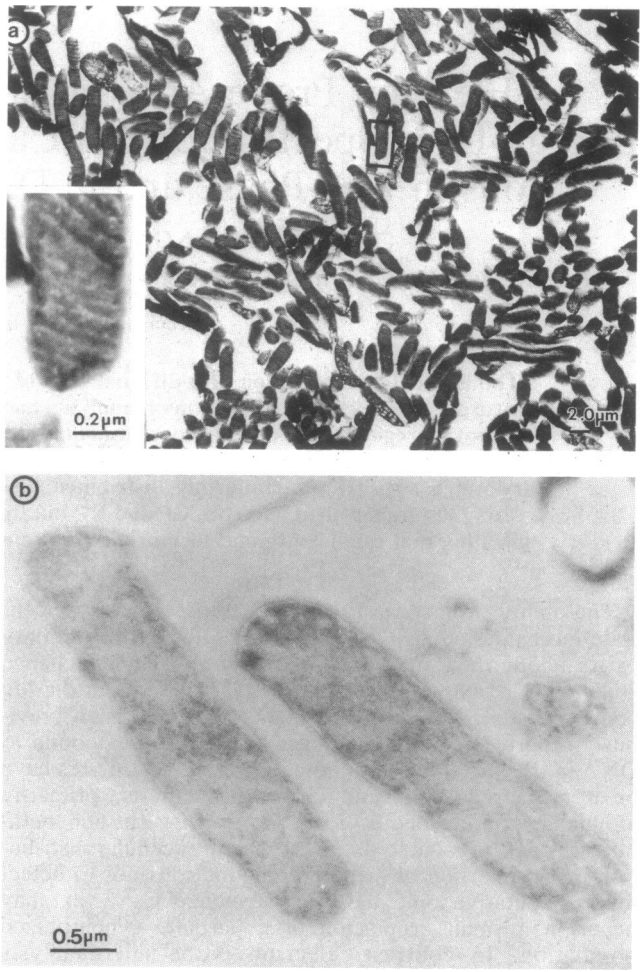

FIG. 2. Conventional transmission of electron micrography (a) of a cryosection of a quick-frozen centrifuged pellet of *E. coli* B prepared as described in the test. Transmission electron microscopy image (b) of a thin section of a specimen frozen as in panel a, but after freezing it was substituted wih ethanol at −80°C and infiltrated with Lowicryl HM-20 at −35°C. Components of the cell wall are visible only in panel b.

EELS. These experiments were also done with the computer-controlled field-emission gun STEM. STEM line-scan spectra across the cell envelope of the *E. coli* were recorded with a 1.0-nm probe focused to a 2.5-nm diameter in 5-nm steps. At each point in the scan, a second difference energy loss spectrum (22) was recorded for 16 s. The calcium and carbon peaks in the second difference were then least-squares fitted to a standard spectrum of known concentration of calcium (23).

RESULTS

The elemental concentrations of log-phase *E. coli* cells are shown in Table 1. The concentration of Mg in the cytoplasm was 205 ± 50.2 mmol/kg (dry weight). Since the intracellular water content in *E. coli* is 1.8 ml/g (dry weight) (7), the Mg

TABLE 2. Elemental concentrations of dividing washed cells of *E. coli* B

Element or ion	Concn (mmol/kg [dry wt] ± SEM)	
	Cytoplasm (n = 28)	Cell envelope (n = 25)
Na	146 ± 7.7	117 ± 5.3
Mg	201 ± 12.5	114 ± 8.3
P	1,543 ± 55.4	1,060 ± 44.4
S	139 ± 11.2	130 ± 9.9
Cl	14.0 ± 1.5	12.0 ± 1.3
K	169 ± 12.8	128 ± 11.3
Ca	32.6 ± 2.2	34.2 ± 2.1

concentration was 114 ± 27.9 mM, in agreement with recent atomic absorption spectroscopic measurements (17), but it was about four times higher than that reported by others (14, 16).

P and Mg were located predominantly in the cytoplasm, and Ca was located predominantly in the cell envelope. The concentrations of Na, Cl, and K in the cytoplasm and in the cell envelope were not significantly different. The calcium concentration in the cell envelope was nearly 25 times higher than that in cytoplasm. We excluded the possibility that the high Ca^{2+} localized to the envelope wall was due to Ca deposited, during the freezing and drying phase, from the extracellular solution. Cells harvested in the log phase were washed with distilled deionized water twice before freezing. The elemental concentrations of washed cells are also shown

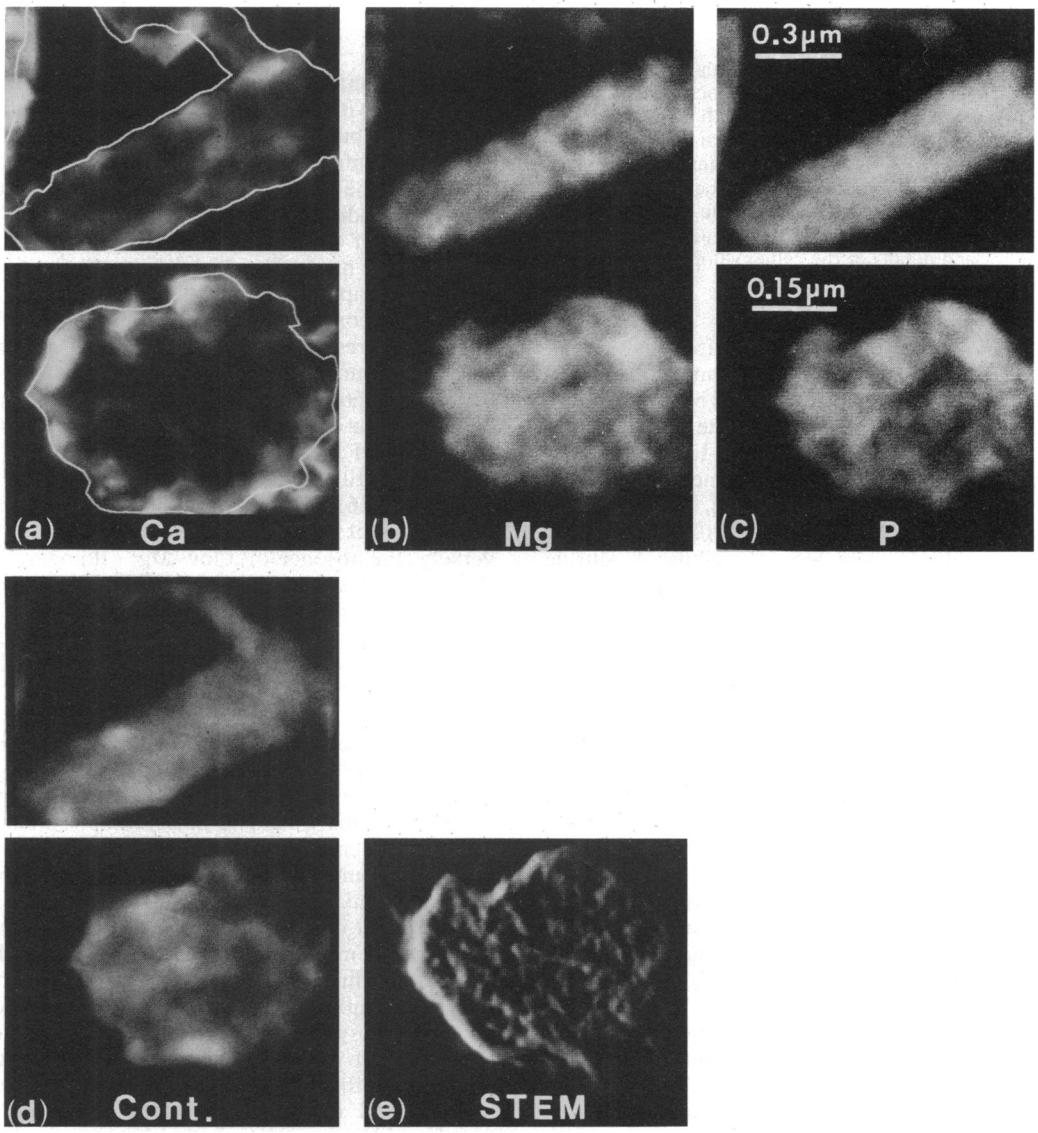

FIG. 3. X-ray maps of transversely (upper panels) or longitudinally (lower panels) sectioned *E. coli*. The relative concentrations of the elements are as follows: Ca, Mg, and P (a, b, and c, respectively) are shown in images composed of 32 × 32 pixels, and an image of the relative mass thickness of the cells, determined from X-ray continuum counts, is shown in panel d. Outlines of the cells from panel d are reproduced in panel a to show the position of Ca with respect to the cell envelope. The electron probe current was 3 nA, and the dwell time for each pixel was 10 s. (e), STEM image of transverse section obtained after X-ray map collection.

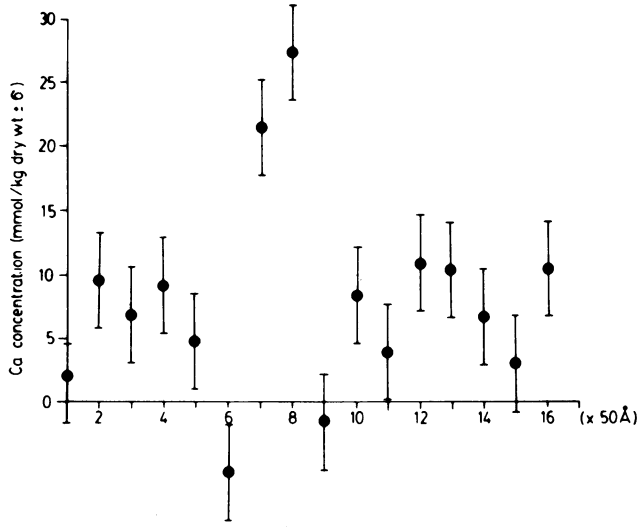

FIG. 4. Calcium concentrations measured with EELS during a computer-controlled STEM line scan, in 5-nm increments, across the cell envelope of a cryosection of *E. coli* B. Each point represents the quantitative results from an energy loss spectrum acquired in 16 s. The specimen was cooled to −100°C during analysis to reduce radiation damage and contamination. The Ca localization region (points 7 and 8) could not be related to a specific structure in the envelope, since dark-field images could not be acquired simultaneously with spectra, and details of the cell envelope were not well defined in unstained cryosections (cf. Fig. 2).

in Table 1. The concentration of Ca localized to the cell envelope was unchanged by washing, indicating that Ca is tightly bound to the envelope. Magnesium in both cytoplasm and cell envelope was also tightly bound. The molar ratio of Ca plus Mg to P in situ (Table 1) was similar to that found in bulk measurements of isolated cytoplasmic membranes of *E. coli* W145 F^- (5). However, during washing, Na, K, and Cl lost two-thirds (Na^+), one-half (K^+), and 9/10 (Cl^-) of their original content (Table 1). The loss of cellular K during washing with cold hypotonic solutions has been previously detected with atomic absorption spectrophotometry (7). Inasmuch as the concentration of monovalent ions in unwashed cells may vary as a function of culture medium, stage of growth (20), and bacterial strain, direct comparison of our results with other studies is difficult. Subject to this qualification, we note that the cellular K content measured in unwashed cells by EPMA was statistically identical with results (617 mmol/kg [dry weight]) of atomic absorption spectrophotometry (7) of wild-type *E. coli*. Cellular Na was higher in the present study, possibly as the result of centrifugation at a low temperature.

In the dividing cells, the cytoplasmic calcium concentration increased and was as high as in the cell wall (Table 2). The data were obtained from washed cells; the cytoplasmic Ca^{2+} was similarly high (29.1 ± 3.3, n = 5) in unwashed dividing cells.

A low average cytoplasmic Ca concentration, measured with large defocused probes, may obscure the presence of high concentrations of localized Ca, i.e., a "hot spot" of Ca could be averaged out by the neighborhood containing low Ca concentrations. Therefore, we used X-ray mapping to display elemental distributions in bacterial cells at a higher spatial resolution and to quantitatively represent the elemental concentrations in the form of optical intensities. Representative X-ray maps of both longitudinally and transversely sectioned cells are shown in Fig. 3. The intensity scales were not set the same for each element. In both figures, it is clearly demonstrated that Ca is localized preferentially in the cell envelope and that Mg is distributed throughout the cytoplasm. Furthermore, at the spatial resolution obtained in these maps (estimated to be about 30 nm because of the Nyquist limit), there is no evidence of compartmentalization of elemental distribution in the cytoplasm.

The relatively high Ca concentrations within the cell envelope of log-phase *E. coli*, detected by EELS in the STEM line-scan mode, is shown in Fig. 4. The sampling distance of the line scan was 5 nm. The error bars are the standard deviations estimated from the statistics of the spectrum. To obtain an equivalent signal-to-noise ratio with X-ray microanalysis data, 800 s per point would be required. The Ca concentrations measured in the cell envelope with EELS and with X-rays are in agreement within the measurement error.

DISCUSSION

The Mg content of *E. coli* measured with EPMA is high, in agreement with the more recent bulk chemical measurements (17), but Mg^{2+} X-ray maps show that this divalent cation is uniformly distributed within the bacterial cell. Therefore, the high Mg content of *E. coli* cannot be ascribed solely to binding to DNA in the nucleoid (17). The spatial resolution of the X-ray maps was clearly sufficient for resolving the nucleoid, which is a relatively distinct and large domain in rapidly frozen bacterial cells (10). A distinctly higher Mg content of such a large (up to about 0.5 μm) domain, if present, would have been easily detected by our mapping parameters. A ready explanation of the uniformly high Mg content of bacterial cells is also apparent from consideration of their ultrastructure, as much of the space not occupied by the nucleoid in the cells is occupied by ribosomes (10). Indeed, the high Mg^{2+} and P content of ribosomes (16, 27) readily explains the uniformly high concentrations of these two elements in the X-ray maps. Conversely, the absence of a low-Mg^{2+} domain in the region of the nucleoid supports the possibility (17) that Mg is also bound to DNA. The fact that the Mg and P content of *E. coli*, unlike its Na, Cl, and K content, did not decrease after washing with distilled water, also supports the conclusion that Mg and P are predominantly present in a tightly bound form.

The identification of individual dividing cells by morphological criteria (3 μm long with an indentation) enabled us to directly measure their ionic composition with electron probe X-ray microanalysis. The most notable finding was a very significant increase in the cytoplasmic Ca^{2+} in dividing cells (Table 2) compared with the low values during log phase (Tables 1 and 2). The fact that the increased cytoplasmic Ca^{2+} content of dividing cells was not detectable by X-ray fluorescence measurements (14) can probably be ascribed to two factors: first, the samples analyzed by the latter method represent a mixture of cells in various phases of growth in an imperfectly synchronized population; second, such bulk measurement would also include the Ca content of the cell membranes that is equally high in all the growth phases, dividing and resting. It will be interesting to determine whether the increased cytoplasmic Ca^{2+} in dividing *E. coli*, observed in our study, plays an initiating or regulatory role in bacterial cell division.

The high Ca^{2+} content of the cell envelope demonstrated in X-ray maps is in agreement with the role of divalent

cations in maintaining the structural organization of the lipopolysaccharide side of outer membrane (15, 18). The EELS line scan (Fig. 4) is the first in situ demonstration of membrane-bound Ca at high (5 nm) resolution. It has been suggested that membrane-bound Ca^{2+} may mediate physiological or pathological changes in *E. coli* (3, 6). We did not resolve in unstained cryosections the constituents of the cell envelope, and it will be interesting to determine how the bound Ca is partitioned between, respectively, the outer lipopolysaccharide (5) component of the cell envelope and the underlying peptidoglycan gel (2, 9, 21). This question and the localization of high-affinity Ca^{2+}-binding proteins in *E. coli* (8) are clearly within the sensitivity and spatial resolution of electron optical methods (see above and references 26 and 28 for review).

ACKNOWLEDGMENTS

This work was supported by Public Health Service grant HL15835 and training grant HL07499 from the National Institutes of Health to the Pennsylvania Muscle Institute (H.S. and A.P.S.) and by Public Health Service grant RR-2483 from the National Institutes of Health to Mid-Atlantic Regional Research Center Intermediate Voltage Electron Microscopy (C.F.C.).

We thank M. Tokito for excellent technical support, including cryoultramicrotomy. We thank H. Davies and E. Sommer for the gift of *E. coli* and E. L. Buhle for his help with image processing.

LITERATURE CITED

1. **Appleton, T. C., K. Johnstone, and D. J. Ellar.** 1980. Location of metal ions in *Bacillus megaterium* spores by high-resolution electron probe X-ray microanalysis. FEBS Lett. **7**:97–101.
2. **Bayer, M. E.** 1974. Ultrastructure and organization of the bacterial envelope. Ann. N.Y. Acad. Sci. **235**:6–28.
3. **Boulanger, P., B. Labedan, and L. Letellier.** 1985. Involvement of calcium in the transient depolarization of *E. coli* cytoplasmic membrane induced by phage adsorption: a study with the fluorescent calcium indicator quin2. Biochem. Biophys. Res. Commun. **131**:856–862.
4. **Chang, C.-F., H. Shuman, and A. P. Somlyo.** 1984. Electron probe analysis, X-ray mapping and electron energy loss spectroscopy of elemental distribution in *Escherichia coli* B, p. 570–571. *In* G. W. Bailey (ed.), Proceedings of the 42nd Annual Meeting of the Electron Microscopy Society of America. San Francisco Press, Inc., San Francisco.
5. **Coughlin, R. T., S. Tonsager, and E. J. McGroarty.** 1983. Quantitation of metal cations bound to membranes and extracted lipopolysaccharide of *Escherichia coli*. Biochemistry **22**:2002–2007.
6. **Elsbach, P., J. Weiss, and L. Kao.** 1985. The role of intramembrane Ca^{2+} in the hydrolysis of the phospholipids of *Escherichia coli* by Ca^{2+}-dependent phospholipases. J. Biol. Chem. **260**:1618–1622.
7. **Epstein, W., and S. G. Schultz.** 1965. Cation transport in *Escherichia coli*. V. Regulation of cation content. J. Gen. Physiol. **49**:221–234.
8. **Harmon, A. C., D. Prasher, and M. J. Cormier.** 1985. High affinity calcium-binding proteins in *Escherichia coli*. Biochem. Biophys. Res. Commun. **127**:31–36.
9. **Hobot, J. A., E. Carlemalm, W. Villiger, and E. Kellenberger.** 1984. Periplasmic gel: new concept resulting from the reinvestigation of bacterial cell envelope ultrastructure by new methods. J. Bacteriol. **160**:143–152.
10. **Hobot, J. A., W. Villiger, J. Escaig, M. Maeder, A. Ryter, and E. Kellenberger.** 1985. Shape and fine structure of nucleoids observed on sections of ultrarapidly frozen and cryosubstituted bacteria. J. Bacteriol. **162**:960–971.
11. **Jasper, P., and S. Silver.** 1977. Magnesium transport in microorganisms, p. 7–47. *In* E. D. Weinberg (ed.), Microorganisms and minerals. Marcel Dekker, Inc., New York.
12. **Kitazawa, T., H. Shuman, and A. P. Somlyo.** 1983. Quantitative electron probe analysis: problems and solutions. Ultramicroscopy **11**:251–262.
13. **Kowarski, D.** 1984. Intelligent interface for a microprocessor controlled scanning transmission electron microscope with X-ray imaging. J. Electron Microsc. Tech. **1**:175–184.
14. **Kung, F.-C., J. Raymond, and D. A. Glaser.** 1976. Metal ion content of *Escherichia coli* versus cell age. J. Bacteriol. **126**:1089–1095.
15. **Leive, L.** 1974. The barrier function of the gram-negative envelope. Ann. N.Y. Acad. Sci. **235**:109–129.
16. **Lusk, J. E., R. J. P. Williams, and E. P. Kennedy.** 1968. Magnesium and the growth of *Escherichia coli*. J. Biol. Chem. **243**:2618–2624.
17. **Moncany, M. L. J., and E. Kellenberger.** 1981. High magnesium content *Escherichia coli* B. Experientia **37**:846–847.
18. **Nikaido, H.** 1973. Biosynthesis and assembly of lipopolysaccharide and the outer membrane layer of gram-negative cell wall, p. 131–208. *In* L. Leive (ed.), Bacterial membranes and walls. Marcel Dekker, Inc., New York.
19. **Rosen, B. P., S. V. Ambudkar, M. G. Bordolla, C. M. Chen, H. L. T. Mobley, H. Tsujibo, and G. W. Zlotnick.** 1984. Calcium, sodium, phosphate, and arsenate transport in cells and vesicles of *Escherichia coli*, p. 219–226. *In* F. Bronner and M. Peterlik (ed.), Epithelial calcium and phosphate transport: molecular and cellular aspects. Alan R. Liss, Inc., New York.
20. **Schultz, S. G., and A. K. Solomon.** 1961. Cation transport in *Escherichia coli*. I. Intracellular Na and K concentrations and net cation movement. J. Gen. Physiol. **45**:355–369.
21. **Shechter, E., and L. Y. Letellier.** 1985. Structural dynamics of the cell membrane, p. 121–160. *In* N. Nanninga (ed.), Molecular cytology of *Escherichia coli*. Academic Press Inc., New York.
22. **Shuman, H., and P. Kruit.** 1985. Quantitative data processing of parallel recorded electron energy-loss spectra with low signal to background. Rev. Sci. Instrum. **56**:231–239.
23. **Shuman, H., P. Kruit, and A. P. Somlyo.** 1983. Quantitative electron energy loss spectroscopy of low concentration of calcium in carbon matrices, p. 247–251. *In* R. Gooley (ed.), Microbeam analysis society. San Francisco Press, Inc., San Francisco.
24. **Shuman, H., A. V. Somlyo, and A. P. Somlyo.** 1976. Quantitative electron probe microanalysis of biological thin sections: method and validity. Ultramicroscopy **1**:317–339.
25. **Silver, S., K. Toth, and H. Scribner.** 1975. Facilitated transport of calcium by cells and subcellular membranes of *Bacillus subtilis* and *Escherichia coli*. J. Bacteriol. **122**:880–885.
26. **Somlyo, A. P.** 1985. Compositional mapping in biology: X-rays and electrons. J. Ultrastruct. Res. **83**:135–142.
27. **Somlyo, A. P., M. Bond, and A. V. Somlyo.** 1985. The calcium content of mitochondria and endoplasmic reticulum in liver rapidly frozen in situ. Nature (London) **314**:622–625.
28. **Somlyo, A. P., and H. Shuman.** 1982. Electron probe and electron energy loss analysis in biology. Ultramicroscopy **8**:219–234.
29. **Somlyo, A. V., and J. Silcox.** 1979. Cryoultramicrotomy for electron probe analysis, p. 535–555. *In* C. Lechene and R. Warner (ed.), Microbeam analysis in biology. Academic Press, Inc., New York.
30. **Stewart, M., A. P. Somlyo, A. V. Somlyo, H. Shuman, J. A. Lindsay, and W. G. Murrell.** 1980. Distribution of calcium and other elements in cryosectioned *Bacillus cereus* T spores, determined by high-resolution scanning electron probe X-ray microanalysis. J. Bacteriol. **143**:481–491.
31. **Stewart, M., A. P. Somlyo, A. V. Somlyo, H. Shuman, J. A. Lindsay, and W. G. Murrell.** 1981. Scanning electron probe X-ray microanalysis of elemental distributions in freeze-dried cryosections of *Bacillus coagulans* spores. J. Bacteriol. **147**: 670–674.